

New Epitaxial Phase Transition between DG and HEX in PS-*b*-PI

Hae-Woong Park,[†] Jueun Jung,[†] Taihyun Chang,^{*,†} Kazuyuki Matsunaga,[‡] and Hiroshi Jinnai^{*,‡}

Department of Chemistry and Polymer Research Institute, Pohang University of Science and Technology, Pohang, 790-784, Korea, and Department of Macromolecular Science and Engineering, Graduate School of Science and Engineering, Kyoto Institute of Technology, Kyoto 606-8585, Japan

Received October 27, 2008; E-mail: tc@postech.ac.kr; hjinnai@kit.ac.jp

Block copolymers undergo order–order phase transitions which often exhibit an epitaxial relationship between the morphology of two phases.^{1–9} One of the extensively studied examples is the phase transition from or to a double gyroid (DG) structure, which is more intriguing than the others due to the structural complexity of the DG phase.^{1–8,10} In this communication, we would like to report on a newly found epitaxial phase transition path between the hexagonally packed cylinder (HEX) and DG structure, which has been studied extensively in block copolymers or in micelles.^{1–4,11} Except for a few cases,⁴ there is a consensus that the phase transition between HEX and DG has an epitaxial relationship between the $\{121\}_{\text{DG}}$ plane and $\{10\}_{\text{HEX}}$ plane and between the $\langle 111 \rangle_{\text{DG}}$ direction and the HEX cylinder axis, respectively.

In most of the previous experimental studies, X-ray or neutron scattering methods were used together with transmission electron microscopy (TEM) for structural analysis. In so doing, macroscopic alignment of the microphase domains were often tried to elucidate the structure more clearly and easily. We used a thin film on a Si wafer substrate, in which $\{121\}_{\text{DG}}$ planes orient parallel to the substrate plane near perfectly after thermal annealing without applying any external field.^{7,8} The internal structure of the thin films was investigated by grazing incidence small-angle X-ray scattering (GISAXS), TEM, and transmission electron microtomography (TEMT) along the phase transition path. GISAXS has been used efficiently to investigate the internal structure of block copolymer thin film.⁷ TEMT is a powerful tool allowing us to observe the 3D-structure directly.^{8,12,13} By virtue of good domain orientation in the thin film and the powerful methods for the structural investigation, we were able to observe the coexisting structure of the DG and HEX phases unambiguously.

To develop the coexisting structures of DG and HEX, the polystyrene-*block*-polyisoprene (PS-*b*-PI) thin films ($M_n = 36\,300$, $M_w/M_n = 1.01$, $f_{\text{PI}} = 0.680$) were annealed at 182 °C for 1 day and subsequently quenched to room temperature to freeze the structures. The ~700 nm thick PS-*b*-PI film was spin-coated onto a silicon wafer. The TEM images and GISAXS patterns of the DG, HEX, and their coexisting phases are presented in Figure S1 in the Supporting Information.

Figure 1 shows a 3D TEMT-image and its digitally sliced images of the DG/HEX transitional structure. In the 3D-image, Figure 1a, only the PS domain is shown and this hexahedral image was taken from the rectangular box area in the TEM image shown in Figure 1b (3D-movie is available in the Supporting Information, Figure S2.) The dimension of the hexahedron is 400, 200, and 80 nm (x , y , z). Here, z is the direction of the incident electron beam, and xz is the film plane (i.e., substrate surface). Figure 1b clearly shows the grain boundary region of the coexisting DG and HEX phases.

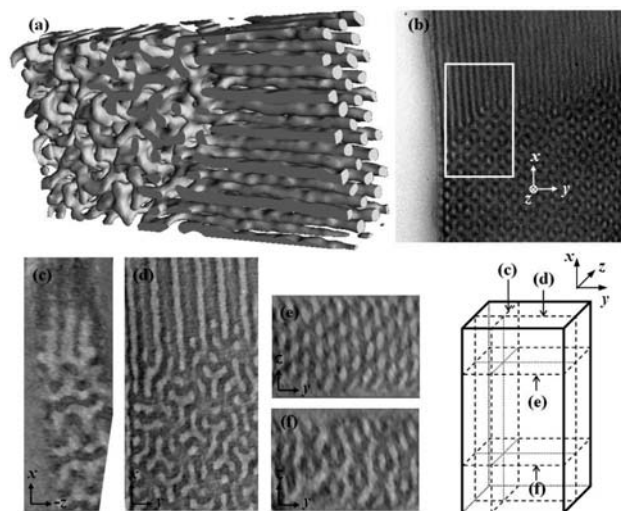


Figure 1. (a) 3D reconstructed image of coexisting structure of DG and HEX. The dimension of the hexahedron is 400, 200, and 80 nm (x , y , z). In this image, only the PS domain is shown. (b) TEM image of the sample region from which the 3D image was reconstructed (boxed area). (c–f) Images of the cross section illustrated in the hexahedron. PI block was stained with OsO_4 and appears darker.

HEX cylinders are oriented along the x axis while the DG phase shows the $\{111\}_{\text{DG}}$ plane characterized by the wagon-wheel-shaped structure.

To better appreciate the 3D-structure of the coexisting morphology of DG and HEX, several digitally sliced images are obtained for the cross section illustrated in the hexahedron. Figure 1e is a view of the HEX grain perpendicular to the cylinder axis while Figure 1f is the image of $\{220\}_{\text{DG}}$, which is orthogonal to both $\{121\}_{\text{DG}}$ and $\{111\}_{\text{DG}}$. It indicates that the HEX cylinder axis is perpendicular to $\{220\}_{\text{DG}}$ and parallel to both $\{121\}_{\text{DG}}$ and $\{111\}_{\text{DG}}$. Figure 1c and d show the images consistent with this picture. Figure 1c shows the coexisting $\{10\}_{\text{HEX}}$ and $\{121\}_{\text{DG}}$. Figure 1d is an expanded version of Figure 1b but more clearly shows coexisting $\{11\}_{\text{HEX}}$ and $\{111\}_{\text{DG}}$ by virtue of being a digitally sliced image. Therefore, it is unambiguously confirmed that $\{121\}_{\text{DG}}$ and $\{111\}_{\text{DG}}$ were respectively converted to $\{10\}_{\text{HEX}}$ and $\{11\}_{\text{HEX}}$, which has not been reported in the earlier works.^{1–3,11}

Matsen reported earlier on how the phase transition between DG and HEX would occur.³ According to his proposal, the $\langle 111 \rangle_{\text{DG}}$ axis is converted to the cylinder axis of HEX. As illustrated in Figure 2a, the projection along the $\langle 111 \rangle_{\text{DG}}$ direction has 3-fold symmetry and the loci corresponding to the HEX cylinder axes are marked with small circles. The dimension of the hexagonal shape on the $\{111\}_{\text{DG}}$ projection is very close to that of the HEX cylinders as mentioned earlier, i.e., $d_{\{121\}_{\text{DG}}} \approx d_{\{10\}_{\text{HEX}}}$. The loci are not structurally uniform but consist of two different kinds as

[†] Pohang University of Science and Technology.

[‡] Kyoto Institute of Technology.

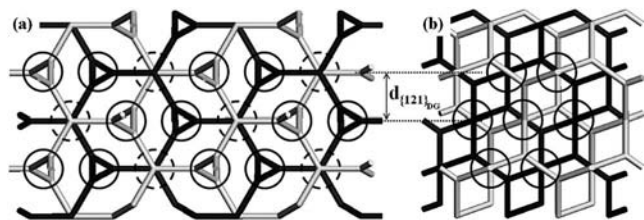


Figure 2. (a) Simulated projection along $\langle 111 \rangle_{\text{DG}}$. Two single gyroids are expressed with different gray tones. The loci of the cylinder axis are marked with circles. There are two different kinds of loci as expressed with solid and dotted circles. (b) Simulated projection along $\langle 220 \rangle_{\text{DG}}$. The loci of the cylinder axis are marked with circles. In this $\langle 220 \rangle_{\text{DG}} \rightarrow$ cylinder axis mechanism, all loci are equivalent.

marked with solid and dotted circles. At the loci marked with dotted circles, tripodal skeletons of two single gyroids need to be connected to form an HEX cylinder. Matsen reasonably explained the DG to HEX conversion of this kind.³ For the other loci marked with solid circles, only a single gyroid skeleton is converted to a cylinder and two single gyroids alternatively form adjacent cylinders. In this case, the gyroid skeletons are already connected (helically rotating to be projected as a triangle) along the cylinder axis. Therefore, each $1/3$ of the HEX cylinders is formed from different DG skeletons: A gyroid, B gyroid, and A+B gyroid (see Figure S3).

In the newly observed transitional structure in this study, the HEX cylinder is formed along the $\langle 220 \rangle_{\text{DG}}$ direction. The symmetry of the $\{220\}_{\text{DG}}$ projection is slightly distorted from the right hexagon as shown in Figure 2b, where the loci of cylinders are marked with circles. In contrast to the $\langle 111 \rangle_{\text{DG}} \rightarrow$ cylinder axis mechanism, all loci are equivalent and the cylinder axis would grow connecting two single gyroid skeletons (see Figure S4). Even though the hexagon is distorted, the $\{121\}_{\text{DG}}$ plane is to be converted to the $\{10\}_{\text{HEX}}$ plane without perturbation. This type of epitaxial transition path has not been recognized in the previous studies. We found this type of conversion, i.e., $\langle 220 \rangle_{\text{DG}} \rightarrow$ cylinder axis, exclusively in the two independently prepared thin film samples used in this study. Nonetheless, we do not exclude the possibility of finding the other epitaxial path reported in the literature, i.e., conversion of $\langle 111 \rangle_{\text{DG}} \rightarrow$ HEX cylinder axis, since TEM observation is not free from the limited number of sampling.

The apparent distinctions of this study from the previous ones are the thin film structure and the direction of phase transition, DG \rightarrow HEX. The distinctive phase transition behaviors in thin film from that of bulk have been reported earlier. Park et al. reported on the phase transition of HPL \rightarrow DG that HPL layers are converted to $\{121\}_{\text{DG}}$ in the thin film⁷ while such an orderly transition was not observed in shear-oriented bulk.^{2,5} More recently Hasegawa and co-workers¹³ reported on the DG/HPL grain boundary structure in bulk that HPL layers are connected to $\{111\}_{\text{DG}}$ which is not compatible with the epitaxial relationship between the HPL layers and $\{121\}_{\text{DG}}$ found in the thin film.⁷ These are good examples indicating that the surface interactions of the block copolymers play an important role for such deviations. In this system, PI blocks preferably wet both interfaces with the Si wafer and air. In addition, most of the previous works used the HEX \rightarrow DG transition since the HEX phase is easier to orient the domains and the aligned HEX structure facilitates the investigation of the structural relationship before and after the phase transition.^{1,2} In this work, we could work

on the DG \rightarrow HEX transition since the DG phase is oriented well in thin films. We are currently working on whether the transition direction can make any difference in the epitaxial phase transition.

In summary, we investigated the phase transition from DG to HEX in thin films and successfully obtained a 3D TEM image of the transitional structure. We found a new epitaxial phase transition path from DG to HEX, which involves epitaxial relations between $\{121\}_{\text{DG}}$ and $\{10\}_{\text{HEX}}$ and between $\{111\}_{\text{DG}}$ and $\{11\}_{\text{HEX}}$. $\{220\}_{\text{DG}}$ becomes the grain boundary plane. Although further studies are needed to clarify why such a new epitaxial transition path was observed exclusively in this study, the newly found path seems to have an advantage over the reported path in such a way that all the HEX cylinders are converted from equivalent structures in DG while the previously reported path involves two different structures in DG.

Acknowledgment. T.C. acknowledges support from KOSEF (R0A-2007-000-20125-0) and the BK 21 program. H.J. is grateful for support from the Ministry of Education, Science, Sports and Culture through Grant-in-Aid No. 19031016. The GISAXS measurements at PAL were supported by the Ministry of Science and Technology and POSCO.

Supporting Information Available: Sample preparation method, movie showing the 3D-image of DG/HEX grain boundary, and supplementary figures for easier understanding of newly observed transition mechanism from DG to HEX. This material is available free of charge via the Internet at <http://pubs.acs.org>.

References

- (1) (a) Schulz, M. F.; Bates, F. S.; Almdal, K.; Mortensen, K. *Phys. Rev. Lett.* **1994**, *73*, 86. (b) Floudas, G.; Ulrich, R.; Wiesner, U. *J. Chem. Phys.* **1999**, *110*, 652. (c) Wang, C. Y.; Lodge, T. P. *Macromolecules* **2002**, *35*, 6997.
- (2) (a) Förster, S.; Khandpur, A. K.; Zhao, J.; Bates, F. S.; Hamley, I. W.; Ryan, A. J.; Bras, W. *Macromolecules* **1994**, *27*, 6922. (b) Vigild, M. E.; Almdal, K.; Mortensen, K.; Hamley, I. W.; Fairclough, J. P. A.; Ryan, A. J. *Macromolecules* **1998**, *31*, 5702.
- (3) Matsen, M. W. *Phys. Rev. Lett.* **1998**, *80*, 4470.
- (4) Honda, T.; Kawakatsu, T. *Macromolecules* **2006**, *39*, 2340.
- (5) Zhao, J.; Majumdar, B.; Schulz, M. F.; Bates, F. S.; Almdal, K.; Mortensen, K.; Hajduk, D. A.; Gruner, S. M. *Macromolecules* **1996**, *29*, 1204.
- (6) (a) Hamley, I. W.; Fairclough, J. P. A.; Ryan, A. J.; Mai, S. M.; Booth, C. *Phys. Chem. Chem. Phys.* **1999**, *1*, 2097. (b) Zhu, L.; Huang, P.; Chen, W. Y.; Weng, X.; Cheng, S. Z. D.; Ge, Q.; Quirk, R. P.; Senador, T.; Shaw, M. T.; Thomas, E. L.; Lotz, B.; Hsiao, B. S.; Yeh, F. J.; Liu, L. Z. *Macromolecules* **2003**, *36*, 3180.
- (7) (a) Park, I.; Lee, B.; Ryu, J.; Im, K.; Yoon, J.; Ree, M.; Chang, T. *Macromolecules* **2005**, *38*, 10532. (b) Lee, B.; Park, I.; Yoon, J.; Park, S.; Kim, J.; Kim, K. W.; Chang, T.; Ree, M. *Macromolecules* **2005**, *38*, 4311.
- (8) (a) Park, H.-W.; Im, K.; Chung, B.; Ree, M.; Chang, T.; Sawa, K.; Jinnai, H. *Macromolecules* **2007**, *40*, 2603. (b) Dohi, H.; Kimura, H.; Kotani, M.; Kaneko, T.; Kitaoka, T.; Nishi, T.; Jinnai, H. *Polym. J.* **2007**, *39*, 749.
- (9) (a) Sakurai, S.; Kawada, H.; Hashimoto, T.; Fetters, L. J. *Macromolecules* **1993**, *26*, 5796. (b) Koppi, K. A.; Tirrell, M.; Bates, F. S.; Almdal, K.; Mortensen, K. *J. Rheol.* **1994**, *38*, 999. (c) Laradji, M.; Shi, A. C.; Noolandi, J.; Desai, R. C. *Macromolecules* **1997**, *30*, 3242. (d) Ryu, C. Y.; Lodge, T. P. *Macromolecules* **1999**, *32*, 7190. (e) Kimishima, K.; Koga, T.; Hashimoto, T. *Macromolecules* **2000**, *33*, 968. (f) Krishnamoorti, R.; Silva, A. S.; Modi, M. A.; Hammouda, B. *Macromolecules* **2000**, *33*, 3803. (g) Matsen, M. W. *J. Chem. Phys.* **2001**, *114*, 8165. (h) Lee, H. H.; Jeong, W. Y.; Kim, J. K.; Ihn, K. J.; Kornfield, J. A.; Wang, Z. G.; Qi, S. Y. *Macromolecules* **2002**, *35*, 785. (i) Lai, C. J.; Loo, Y. L.; Register, R. A.; Adamson, D. H. *Macromolecules* **2005**, *38*, 7098. (j) Ahn, J. H.; Zin, W. C. *Macromol. Res.* **2003**, *11*, 152.
- (10) Jinnai, H.; Nishikawa, Y.; Spontak, R. J.; Smith, S. D.; Agard, D. A.; Hashimoto, T. *Phys. Rev. Lett.* **2000**, *84*, 518.
- (11) (a) Rangon, Y.; Charvolin, J. *J. Phys. Chem.* **1988**, *92*, 2646. (b) Clerc, M.; Levelut, A. M.; Sadoc, J. F. *J. Phys. II France* **1991**, *1*, 1263.
- (12) Jinnai, H.; Nishikawa, Y.; Ikehara, T.; Nishi, T. *Adv. Polym. Sci.* **2004**, *170*, 115.
- (13) Mareau, V. H.; Akasaka, S.; Osaka, T.; Hasegawa, H. *Macromolecules* **2007**, *40*, 9032.

JA808259M